

Blind Source Separation-Enabled Joint Communication and Sensing in IBFD MIMO Systems

Siyao Li, Conrad Prisby, Thomas Yang

Department of Electrical Engineering and Computer Science,
Embry-Riddle Aeronautical University, Daytona Beach, FL, USA

E-mail: lis14@erau.edu, prisbyc@my.erau.edu, yang482@erau.edu

Abstract—This paper addresses the challenge of joint communication and sensing (JCAS) in next-generation wireless networks, with an emphasis on in-band full-duplex (IBFD) multiple-input multiple-output (MIMO) systems. Traditionally, self-interference (SI) in IBFD systems is a major obstacle to recovering the signal of interest (SOI). Under the JCAS paradigm, however, this high-power SI signal presents an opportunity for efficient sensing. Since each transceiver node has access to the original SI signal, its environmental reflections can be exploited to estimate channel conditions and detect changes, without requiring dedicated radar waveforms. We propose a blind source separation (BSS)-based framework to simultaneously perform self-interference cancellation (SIC) and extract sensing information in IBFD MIMO settings. The approach applies the Fast Independent Component Analysis (FastICA) algorithm to separate the SI and SOI signals while enabling simultaneous signal recovery and channel estimation. Simulation results confirm the framework's effectiveness, showing improved sensing and communication performance as signal frame size increases.

Index Terms—MIMO, IBFD, channel estimation, joint communication and sensing, blind source separation.

I. INTRODUCTION

The rapid growth of mobile data traffic and the shift toward millimeter-wave (mmWave) communication necessitate an evolution in wireless technologies to meet increasing bandwidth demands [1]. However, spectrum scarcity remains a major challenge, limiting the capacity to support high data rates, as reflected in the soaring cost of spectrum allocation [2]. To enhance spectral efficiency and resource utilization, in-band full-duplex (IBFD) multiple-input multiple-output (MIMO) wireless communications have gained significant attention [3], [4], which allows a wireless transceiver to transmit and receive data simultaneously using the same frequency band. Nevertheless, a major challenge for IBFD systems is managing self-interference (SI), the leakage of a node's own transmitted signal into its receiver chain, which can overshadow the weaker signal of interest (SOI).

The integration of joint communication and sensing (JCAS) is particularly aligned with emerging military requirements for FutureG and beyond [5]. Modern defense operations demand resilient, spectrum-efficient systems capable of simultaneously maintaining covert, jam-resistant communications while providing situational awareness. By

reusing the SI signal as a sensing probe, IBFD JCAS systems reduce electromagnetic signature, conserve bandwidth, and enable real-time detection of environmental changes such as adversarial jamming, drone surveillance, or battlefield mobility [6]. These dual-use capabilities highlight the timeliness of JCAS for defense-oriented applications, where spectrum agility, stealth, and multifunctionality are critical (e.g., see [7]–[14] and references therein).

Existing approaches to sensing often rely on deterministic reference signals [15], [16], while communication employs random modulation schemes such as QAM or BPSK. From an information-theoretic perspective, treating these functionalities separately is suboptimal [17]. Instead, integrating sensing with communication at the physical layer has the potential to significantly improve efficiency and reduce hardware and energy overhead.

Recent research has increasingly focused on leveraging blind source separation (BSS) techniques for JCAS within IBFD MIMO frameworks. A comprehensive survey outlines BSS applications in adaptive wireless systems, demonstrating its potential for handling overlapping signals in MIMO-based cognitive radios and spectrum sensing contexts [18]. A sparsity-enhanced source separation scheme is proposed in [19] to mitigate aliasing in joint communication and radar scenarios. Fouda et al. [20] further explored the design of BSS architectures tailored for full-duplex systems, emphasizing the challenges associated with maintaining computational efficiency while managing strong SI signals. Barneto [21] provides insights into waveform and hardware integration strategies, offering a foundational understanding of signal co-design in cellular JCAS systems.

Contributions: Despite these advances, few works have examined the use of BSS in settings where the SI signal is known and can be repurposed for environmental sensing. This paper addresses this gap by applying classical BSS methods in a scenario optimized for practical JCAS deployment. Specifically, we apply the Fast Independent Component Analysis (FastICA) algorithm [22] to decompose the received signal into its constituent sources, enabling both self-interference cancellation (SIC) and environmental sensing. Our contributions thus extend existing work by

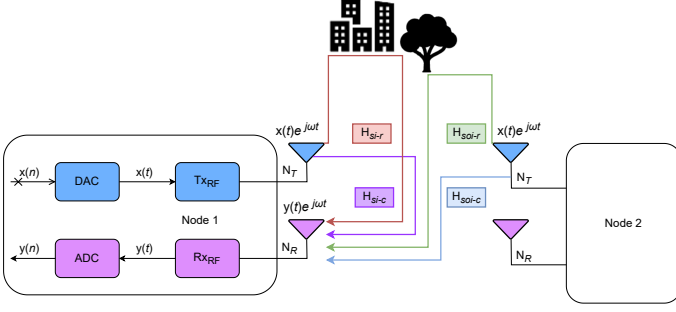


Fig. 1: IBFD system model.

demonstrating a computationally efficient approach to JCAS that balances spectral efficiency, channel estimation accuracy, and system simplicity. We validate the proposed framework through simulations under practical conditions, evaluating performance based on estimation accuracy, signal separation, and convergence behavior. Results demonstrate that our BSS-based solution provides effective joint sensing and communication with minimal overhead, making it a strong candidate for future full-duplex wireless systems.

Organization: The remainder of this paper is organized as follows. Section II introduces the system model. Section III presents the BSS algorithm. Section IV evaluates the performance with numerical examples. Section V concludes this work and discusses future endeavors.

Notations: We use $\mathbb{E}[X]$ to represent the expectation of the random variable X . Let bold letter \mathbf{X} denote a vector or matrix. $\|\cdot\|^2$ represents the Frobenius norm. $\mathcal{N}(\mu, \sigma^2)$ denotes Gaussian distribution with mean μ and variance σ^2 . $\mathbf{M}^{n \times m}$ represents a generic matrix with n rows and m columns.

II. SYSTEM MODEL

As illustrated in Fig. 1, we consider an IBFD MIMO system comprising two transceiver nodes, each equipped with n transmit antennas and m receive antennas. Both nodes simultaneously transmit and receive signals over the same frequency band, enabling full-duplex communication. The received signal at each node is composed of multiple components: (1) the SOI, which includes both direct-path and reflected components from the remote node; and (2) the SI signal, which includes direct leakage between the local transmit and receive antennas and reflections from the environment. Let $R_l(k)$ denote the frequency-domain received signal at the l -th receive antenna at time k . It is expressed as:

$$R_l(k) = \sum_{i=1}^n (H_{si-c}^i(k) + H_{si-r}^i(k)) S_{si}^i(k) + \sum_{i=1}^n (H_{soi-c}^i(k) + H_{soi-r}^i(k)) S_{soi}^i(k) + N(k), \quad l \leq m. \quad (1)$$

Here, $N(k) \sim \mathcal{N}(0, \sigma^2)$ is the additive Gaussian noise; $H_{si-c}^i(k)$ and $H_{soi-c}^i(k)$ are the direct SI and SOI channels

respectively; $H_{si-r}^i(k)$ and $H_{soi-r}^i(k)$ denote the reflected channels at the i -th transmit antenna the discrete time instant k ; $S_{si}^i(k)$ and $S_{soi}^i(k)$ are the SI and SOI signals from the i -th transmit antenna respectively. Each channel matrix is assumed to have independent, identically distributed (i.i.d.) entries. For convenience, we can drop the time index and rewrite (1) in matrix form as

$$\mathbf{R} = (\mathbf{H}_{si-c} + \mathbf{H}_{si-r})\mathbf{S}_{si} + (\mathbf{H}_{soi-c} + \mathbf{H}_{soi-r})\mathbf{S}_{soi} + \mathbf{N}, \quad (2)$$

where $\mathbf{H}_{si-c}, \mathbf{H}_{si-r}, \mathbf{H}_{soi-c}, \mathbf{H}_{soi-r} \in \mathbf{M}^{m \times n}$, $\mathbf{S}_{si}, \mathbf{S}_{soi} \in \mathbf{M}^{n \times 1}$, and $\mathbf{R} \in \mathbf{M}^{m \times 1}$. In particular, \mathbf{H}_{si-c} is the direct self-interference channel, which is in general known to the receiver¹. In this work, we use \mathbf{H}_{si-r} to characterize the reflected channel containing the sensing information. Note that \mathbf{S}_{si} is the transmitted signal from the same node, implying that \mathbf{S}_{si} is known to the receiver. We can further rewrite (2) in the matrix form:

$$\begin{bmatrix} \mathbf{S}_{si} \\ \mathbf{R} \end{bmatrix} = \mathbf{H} \begin{bmatrix} \mathbf{S}_{si} \\ \mathbf{S}_{soi} \end{bmatrix} + \begin{bmatrix} \mathbf{0} \\ \mathbf{N} \end{bmatrix}, \quad (3)$$

where \mathbf{H} is a composite mixing matrix defined as:

$$\mathbf{H} = \begin{bmatrix} \mathbf{I} & \mathbf{0} \\ \mathbf{H}_{si} & \mathbf{H}_{soi} \end{bmatrix} \in \mathbf{M}^{2m \times 2n}, \quad (4)$$

$$\mathbf{H}_{si} = \mathbf{H}_{si-c} + \mathbf{H}_{si-r}, \quad (5)$$

$$\mathbf{H}_{soi} = \mathbf{H}_{soi-c} + \mathbf{H}_{soi-r}, \quad (6)$$

and \mathbf{I} is the identity matrix of size $m \times n$. This formulation in (3) represents a canonical BSS model [23], where known and unknown sources are mixed via partially known channels. The key idea in this paper is to exploit knowledge of the SI signal \mathbf{S}_{si} and its direct channel \mathbf{H}_{si-c} to estimate both the reflection component \mathbf{H}_{si-r} and the unknown communication signal \mathbf{S}_{soi} .

III. BSS BASED CHANNEL ESTIMATION

We now describe the application of the FastICA algorithm [22] to separate the SI and SOI components from the observed signals. For simplicity, we assume $m = n$, meaning each node has an equal number of transmit and receive antennas. The goal is twofold: (1) to estimate the unknown communication signal \mathbf{S}_{soi} for data recovery, and (2) to estimate the reflected SI channel \mathbf{H}_{si-r} for environmental sensing. We treat the sum \mathbf{H}_{soi} in (6) as the overall channel coefficient of the SOI. Given that both the SI signal \mathbf{S}_{si} and the SI direct channel \mathbf{H}_{si-c} are known, we aim to estimate \mathbf{H}_{si-r} , the SI reflection channel, as well as the communication signal \mathbf{S}_{soi} .

¹In practical IBFD systems, the direct SI channel is dominated by the line-of-sight path between the transmitter and receiver antennas of the same node, and primarily depends on the fixed and deterministic hardware characteristics of the transceiver. It can be estimated offline during system calibration or periodically updated using pilot signals. Since the transceiver layout remains unchanged, \mathbf{H}_{si-c} remains relatively stable over time, allowing the receiver to effectively use it for self-interference cancellation techniques.

A. Blind Source Separation for Sensing

The FastICA algorithm exploits non-Gaussianity in the received signal mixture to estimate the independent source components iteratively. The algorithm follows these key steps:

- 1) Preprocessing: Centering and whitening the received signal \mathbf{R} to eliminate correlations.
- 2) Iterative Estimation: Maximize negentropy to extract statistically independent sources.
- 3) Source Recovery: Estimate the unknown channel $\hat{\mathbf{H}}_{\text{si-r}}$ and signal $\hat{\mathbf{S}}_{\text{soi}}$ from the separated components.

B. Performance Metrics

We evaluate the quality of channel estimation using the ergodic linear minimum mean squared error (ELMMSE), which quantifies the average estimation error of the sensed channel:

$$\text{ELMMSE} = \mathbb{E}[\|\mathbf{H}_{\text{si-r}} - \hat{\mathbf{H}}_{\text{si-r}}\|^2]. \quad (7)$$

The communication performance is quantified via the signal-to-residual-error ratio (SRER) of the extracted communication signal:

$$\text{SRER} = \frac{\mathbb{E}[\|\mathbf{S}_{\text{soi}}\|^2]}{\mathbb{E}[\|\mathbf{S}_{\text{soi}} - \hat{\mathbf{S}}_{\text{soi}}\|^2]}. \quad (8)$$

A higher SRER implies more effective signal separation and cleaner communication signal extraction, directly reflecting the system's communication performance under the JCAS paradigm. Additionally, we can assess the ELMMSE of the overall SOI channel \mathbf{H}_{soi} as

$$\text{ELMMSE} = \mathbb{E}[\|\mathbf{H}_{\text{soi}} - \hat{\mathbf{H}}_{\text{soi}}\|^2], \quad (9)$$

which accounts for both the direct transmission channel between the transmitter and receiver, as well as the reflected and scattered components from the surrounding environment. This CSI can be leveraged to optimize the transmission schemes (e.g., precoder design in MIMO systems and optimizing the transmitted signal \mathbf{S}_{soi}), and to maximize the signal-to-interference-plus-noise ratio (SINR)

$$\text{SINR} = \frac{\mathbb{E}[\|\mathbf{H}_{\text{soi}}\mathbf{S}_{\text{soi}}\|^2]}{\mathbb{E}[\|\mathbf{H}_{\text{si}}\mathbf{S}_{\text{si}}\|^2] + \mathbb{E}[\|\mathbf{N}\|^2]}.$$

In Section IV, we also track the number of iterations required for the FastICA algorithm to converge, which provides insight into the computational complexity and algorithmic efficiency of the proposed BSS approach under different signal block sizes. By utilizing these metrics, we provide a comprehensive evaluation framework that jointly characterizes sensing accuracy, communication quality, and transmission efficiency in IBFD MIMO systems.

IV. SIMULATION AND DISCUSSION

A. Simulation Setup

In this section, we evaluate the sensing and communication performance of the proposed system through numerical simulations based on a practical system model. Each node is equipped with two antennas. The reflected channel $\mathbf{H}_{\text{si-r}}$ is modeled as a Rician channel with $\mathbf{H}_{\text{si-r}} \sim \text{Rice}(x, y)$, capturing the presence of a dominant line-of-sight (LOS) component alongside multipath. In contrast, the overall communication channel \mathbf{H}_{soi} is modeled as Rayleigh distributed, representing rich-scattering, non-LOS propagation environments.

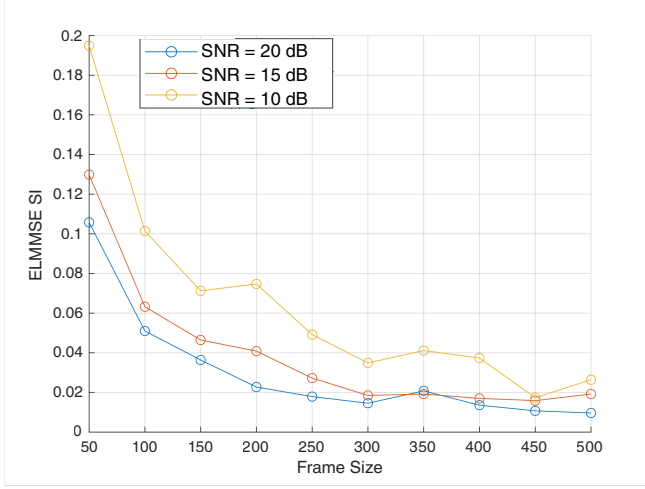
The transmitted signals \mathbf{S}_{si} and \mathbf{S}_{soi} are BPSK modulated, with each symbol randomly chosen from $\{-1, +1\}$. The combined source matrix is defined as $\mathbf{S} = [\mathbf{S}_{\text{si}}; \mathbf{S}_{\text{soi}}] \in \mathbb{R}^{4 \times N}$, where N denotes the frame size (signal processing block length). The received signal is generated by linearly mixing the source signals through the corresponding channel matrices and adding Gaussian noise.

Noise samples are generated from a zero-mean Gaussian distribution with variances $\sigma^2 = 0.01, 0.0316$, and 0.1 , corresponding to signal-to-noise ratios (SNRs) of 20 dB, 15 dB, and 10 dB, respectively. These SNR values reflect low, moderate, and high noise environments. The FastICA algorithm is then applied to recover the sources, using kurtosis as the objective function to be maximized and a convergence threshold of $\epsilon = 10^{-6}$. Each simulation configuration is repeated over 1000 independent trials, and the average results are reported. The frame size is varied from 50 to 500 in increments of 50 to study performance across a broad range of processing lengths.

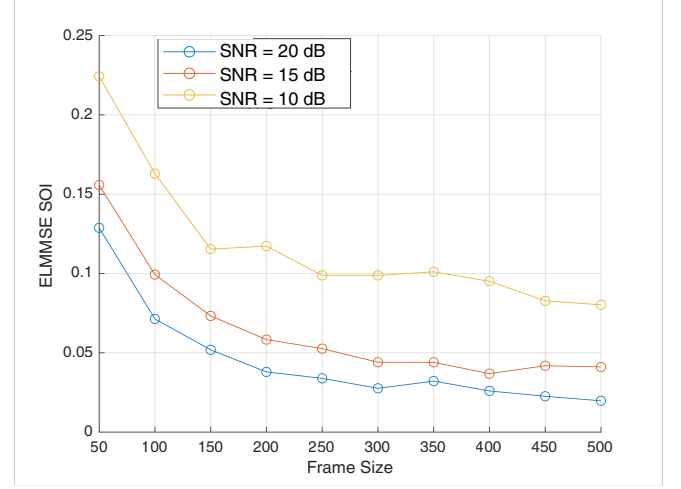
B. Simulation Results

Fig. 2 illustrates the system's performance as a function of frame size and SNR level. The subfigures correspond to different SNR settings, 20 dB, 15 dB, and 10 dB, demonstrating the system's robustness under varying noise conditions.

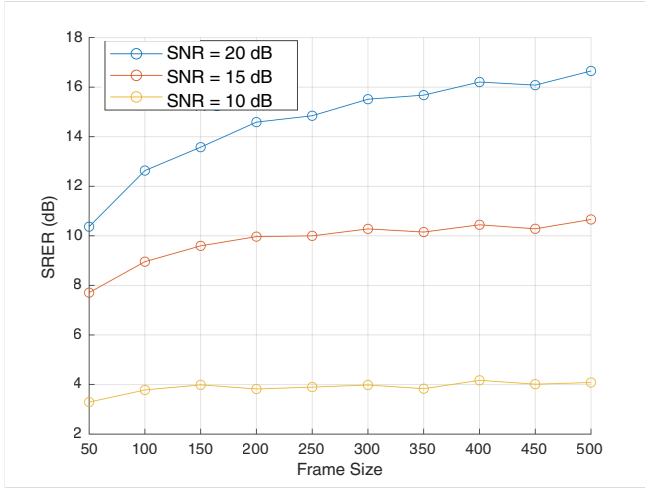
Fig. 2a presents the evolution of the ELMMSE for the SI channel $\mathbf{H}_{\text{si-r}}$ as frame size increases. The results show a consistent decrease in estimation error, highlighting the benefit of larger frame sizes in improving sensing accuracy. A similar trend is observed in Fig. 2b for the communication channel \mathbf{H}_{soi} . In both cases, lower SNRs lead to higher ELMMSE values, indicating increased difficulty in accurate channel estimation. Fig. 2c shows the SRER in decibels, which reflects the quality of recovered communication signals. SRER improves steadily with frame size, particularly under higher SNRs. At 10 dB SNR, the SRER improvement is less pronounced due to strong noise. Fig. 2d depicts the number of iterations required by the FastICA algorithm to converge. For short frame sizes, even a modest increase in the frame size leads to a significant improvement in convergence speed. As the frame size continues to increase, the number of iterations required for convergence gradually decreases at a slower rate, forming a gently sloping trend.



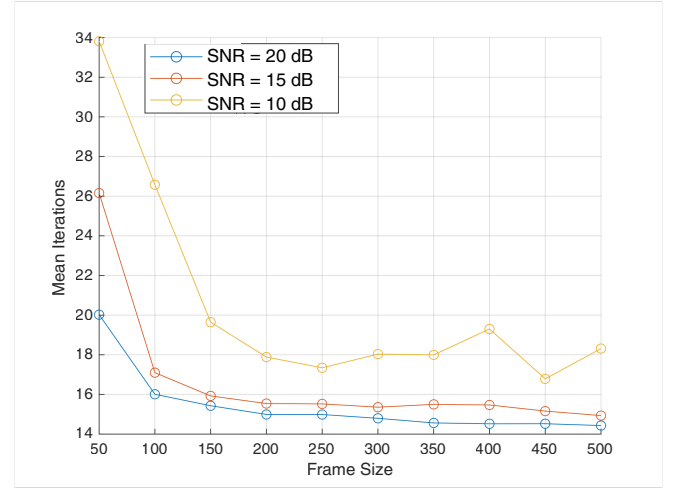
(a) ELMSE of channel sensing $\hat{\mathbf{H}}_{\text{si-r}}$ v.s. frame size.



(b) ELMSE of channel sensing $\hat{\mathbf{H}}_{\text{soi}}$ v.s. frame size.



(c) SRER for SOI in dB v.s. frame size.



(d) Iterations required for convergence v.s. frame size.

Fig. 2: BSS-enabled JCAS performance

The average number of iterations required for convergence is directly influenced by the SNR, i.e., higher SNR levels lead to faster convergence with fewer iterations, while lower SNR conditions increase the number of iterations due to the greater difficulty in signal separation under noisy environments.

The performance improvements observed across all evaluated metrics are attributed to the increased accuracy in signals' statistical property estimation for the FastICA algorithm when a greater number of data samples are available. As the frame size grows, more accurate signal separation and channel estimation are achieved, together with faster convergence speed. However, beyond a certain threshold, approximately 350 symbols per frame, the rate of improvement begins to plateau, indicating diminishing returns with further increases in frame size. This insight is informative for the choice of appropriate frame sizes, especially for communication systems operating in rapidly changing channel environments, when smaller frame sizes may be advantageous due to

the performance degradation caused by changes in channel parameters within each frame.

C. Discussion on the BSS in IBFD MIMO JCAS

The complexity of the FastICA algorithm is generally given by $\mathcal{O}(m^3 + km^2N)$, where m is the number of sources to be separated (in our model, this corresponds to the combined number of transmit antennas from both nodes), N is the frame size, and k is the number of iterations until convergence. In our simulated system, the number of antennas ($m = 4$) is small, making the $\mathcal{O}(m^3)$ term, associated with the initial whitening process, negligible. The dominant factor is the iterative estimation process. Our simulation result in Fig. 2d shows that the number of iterations for convergence is modest and decreases as the frame size increases from 50 to 200 symbols. For a frame size of 350 symbols, the algorithm converges in fewer than 18 iterations on average, even at a low SNR of 10 dB. In practical terms, FastICA is

well-suited for real-time implementation on modern digital signal processors (DSPs) or GPU platforms, particularly when antenna dimensions are modest (e.g., $m \leq 8$).

The integration of BSS techniques into IBFD MIMO systems for JCAS offers compelling advantages that align with the goals of next-generation wireless systems. One of the most significant benefits of such JCAS method is the elimination of dedicated sensing signals. Since the SI signal is already transmitted and fully known at the node, it can be repurposed for environmental sensing, transforming a traditionally detrimental component into a valuable asset. This not only simplifies system design but also reduces the overhead associated with conventional radar signal transmission. Another key advantage lies in the improved spectral efficiency that naturally arises from the JCAS paradigm. By enabling simultaneous communication and sensing within the same frequency band, the proposed IBFD systems avoid the need for additional bandwidth allocation, making more efficient use of the limited spectrum. Furthermore, since BSS methods operate by exploiting statistical independence of source signals, they are able to effectively separate sources without requiring explicit channel state information. In this work, we assume static channel conditions, leaving the dynamic scenarios for future study.

V. CONCLUSION AND FUTURE WORK

In this work, we proposed a blind source separation (BSS)-based framework to enable joint communication and sensing in in-band full-duplex MIMO systems. Leveraging the fully known self-interference signal, our approach repurposes the self-interference signal for environmental sensing, eliminating the need for additional sensing waveforms. We formulated the signal model as a BSS problem and applied the FastICA algorithm to separate the self-interference signal from the signal of interest, with simultaneous channel estimation. Simulation results confirm that the proposed method is fully capable of joint sensing and communication. Also, it was found that while the system performance improves with increasing frame size, the improvement plateaus beyond a certain frame size.

In this study, we focused on a simplified scenario with BPSK source signals. Our framework can be naturally extended to more practical modulation schemes such as QPSK and QAM, where the source signals are complex-valued. This extension will necessitate the use of complex-valued BSS algorithms. Future work will also explore the application of the proposed method to dynamic time-varying channels, which pose many challenges to wireless communication systems. In such scenarios, while longer frames enable more accurate estimation of signals' statistical properties (which translates to improved signal separation performance in static channel conditions), long frame sizes cause degradation of BSS performance in fast-changing channel conditions, because the mixing matrix changes within each individual frame. This issue not only affects signal separation accuracy,

but may also cause some BSS algorithms (such as Fast-ICA) not able to converge. Therefore, the selection of the frame size employed in BSS algorithms becomes critical, and BSS algorithms specifically designed for operation in dynamic mixing processes are desirable. For such scenarios, we will explore the integration of reinforcement learning-based mechanisms to adaptively select optimal frame sizes based on real-time channel dynamics.

REFERENCES

- [1] R. W. Heath, N. Gonzalez-Prelcic, S. Rangan, W. Roh, and A. M. Sayeed, "An overview of signal processing techniques for millimeter wave mimo systems," *IEEE journal of selected topics in signal processing*, vol. 10, no. 3, pp. 436–453, 2016.
- [2] "Belgium completes 5g spectrum auction," <https://5gobservatory.eu/detailed-country-profiles/belgium/>, European 5G Observatory, 2022, online.
- [3] K. E. Kolodziej, *In-Band Full-Duplex Wireless Systems Handbook*. Artech House, 2021.
- [4] H. Alves, T. Riihonen, and H. A. Suraweera, *Full-duplex communications for future wireless networks*. Springer, 2020.
- [5] D. Wen, Y. Zhou, X. Li, Y. Shi, K. Huang, and K. B. Letaief, "A survey on integrated sensing, communication, and computation," *IEEE Communications Surveys & Tutorials*, 2024.
- [6] B. Smida, G. C. Alexandropoulos, T. Riihonen, and M. A. Islam, "In-band full-duplex mimo systems for simultaneous communications and sensing: Challenges, methods, and future perspectives," *arXiv preprint arXiv:2410.06512*, 2024.
- [7] J. A. Zhang, M. L. Rahman, K. Wu, X. Huang, Y. J. Guo, S. Chen, and J. Yuan, "Enabling joint communication and radar sensing in mobile networks—a survey," *IEEE Communications Surveys & Tutorials*, vol. 24, no. 1, pp. 306–345, 2022.
- [8] S. Li and G. Caire, "On the capacity of "beam-pointing" channels with block memory and feedback: The binary case," in *2022 56th Asilomar Conference on Signals, Systems, and Computers*. IEEE, 2022, pp. 1262–1268.
- [9] —, "On the capacity and state estimation error of binary "beam-pointing" channels with block memory and feedback," in *2023 IEEE International Symposium on Information Theory (ISIT)*. IEEE, 2023, pp. 2571–2576.
- [10] X. Fang, W. Feng, Y. Chen, N. Ge, and Y. Zhang, "Joint Communication and Sensing Toward 6G: Models and Potential of Using MIMO," *IEEE Internet of Things Journal*, vol. 10, no. 5, pp. 4093–4116, 2023.
- [11] S. Li, F. Pedraza, and G. Caire, "On the capacity of gaussian "beam-pointing" channels with block memory and feedback," in *2024 IEEE International Symposium on Information Theory (ISIT)*. IEEE, 2024, pp. 2371–2376.
- [12] Y. Song, F. Pedraza, S. Li, S. Li, H. Yu, and G. Caire, "Compressed sensing inspired user acquisition for downlink integrated sensing and communication transmissions," in *ICC 2024 - IEEE International Conference on Communications*, 2024, pp. 5293–5298.
- [13] F. Liu, Y. Cui, C. Masouros, J. Xu, T. X. Han, Y. C. Eldar, and S. Buzzi, "Integrated sensing and communications: Towards dual-functional wireless networks for 6g and beyond," *IEEE Journal on Selected Areas in Communications*, pp. 1–1, 2022.
- [14] M. Ahmadi-pour, M. Kobayashi, M. Wigger, and G. Caire, "An information-theoretic approach to joint sensing and communication," *IEEE Transactions on Information Theory*, pp. 1–1, 2022.
- [15] Z. Wei, Y. Wang, L. Ma, S. Yang, Z. Feng, C. Pan, Q. Zhang, Y. Wang, H. Wu, and P. Zhang, "5G PRS-based sensing: A sensing reference signal approach for joint sensing and communication system," *IEEE Trans. Veh. Technol.*, vol. 72, no. 3, pp. 3250–3263, Mar. 2022.
- [16] I. Bekkerman and J. Tabrikian, "Target detection and localization using MIMO radars and sonars," *IEEE Trans. Signal Process.*, vol. 54, no. 10, pp. 3873–3883, Oct. 2006.
- [17] A. Lapidoth and P. Narayan, "Reliable communication under channel uncertainty," *IEEE transactions on Information Theory*, vol. 44, no. 6, pp. 2148–2177, 1998.

- [18] Z. Luo, C. Li, and L. Zhu, "A comprehensive survey on blind source separation for wireless adaptive processing: Principles, perspectives, challenges and new research directions," *IEEE Access*, vol. 6, pp. 66 685–66 708, 2018.
- [19] B. Jin, J. Sun, P. Ye, F. Zhou, H. Lim, Q. Wu, and N. Al-Dhahir, "Data-driven sparsity-based source separation of the aliasing signal for joint communication and radar systems," *IEEE Transactions on Vehicular Technology*, vol. PP, pp. 1–13, 01 2022.
- [20] M. E. Fouda, C.-A. Shen, and A. E. Eltawil, "Blind source separation for full-duplex systems: Potential and challenges," *IEEE Open Journal of the Communications Society*, vol. 2, pp. 1379–1389, 2021.
- [21] C. Baquero Barneto, *Analysis and Design of Joint Communication and Sensing for Wireless Cellular Networks*, ser. Tampere University Dissertations - Tampereen yliopiston väitöskirjat. Tampere University, 2022.
- [22] E. Bingham and A. Hyvärinen, "A fast fixed-point algorithm for independent component analysis of complex valued signals," *International journal of neural systems*, vol. 10, no. 01, pp. 1–8, 2000.
- [23] H. O. B. S. S. Independent, "Handbook of blind source separation independent component analysis and applications."